Available online at www.sciencedirect.com
SCIENCE DIRECT®
Physica C 425 (2005) 37–43
PHYSICA C
www.elsevier.com/locate/physc

Thermal treatment effect of the oxidized $La_2CuO_{4+\delta}$: The access of continuous and discontinuous T_c

L.H. Liu [a,b,*], G.C. Che [b], J. Zhao [b], Z.X. Zhao [b]

[a] *Physics Department, University of Science and Technology Beijing, Beijing 100083, China*
[b] *National Laboratory for Superconductivity, Institute of Physics, Chinese Academy of Science, P.O. Box 603 Beijing, 100080, China*

Received 19 November 2004; received in revised form 5 May 2005; accepted 18 May 2005
Available online 5 July 2005

Abstract

Superconductive $La_2CuO_{4+\delta}$ with $T_c \sim 40$ K has been obtained by chemical oxidation using NaClO solution. The oxygen-decrease processes have been studied during the thermal treatment processes at different temperatures. The material separates into discrete phases with different transition temperatures for samples treated at 100 °C, consistent with the oxygenation process reported previously. However, T_c decreases continuously in samples treated at 300 °C, similar to the superconducting properties of $La_{2-x}Sr_xCuO_4$. In addition, the coexistence of superconducting and antiferromagnetic phases cannot be observed in our samples. The interrelation between the transition temperature and the treatment conditions such as temperature and time is discussed.

PACS: 74.72.Dn; 74.62.−c

Keywords: Superconductivity; La-based cuprates; Transition temperature variations

1. Introduction

The stoichiometic antiferromagnetic La_2CuO_4 can be transformed into superconductor by introduction of excess oxygen into interstitial sites in the LaO layers. The most popular methods to intercalate extra oxygen are high-pressure, electrochemical and chemical oxidation. For all those oxidation methods, the phase diagram was the object of intense study. In all kinds of phase diagrams, it is well accepted that several superconducting transitions as well as macroscopic phase separation appear due to the mobility of the interstitial oxygen [1–11]. For $0.01 \leqslant \delta \leqslant 0.055$ a miscibility gap exists in which the samples decompose into an oxygen-rich phase with $T_c \sim 30$ K and a

* Corresponding author. Tel.: +86 0186 8116 6855; fax: +86 0186 8264 9531.
E-mail address: lhliu@sas.ustb.edu.cn (L.H. Liu).

0921-4534/$ - see front matter © 2005 Elsevier B.V. All rights reserved.
doi:10.1016/j.physc.2005.05.014

stoichiometric antiferromagnetic La_2CuO_4 phase. At higher doping level $\delta > 0.055$, the system shows rich superconducting phases with T_c of 15, 30–32 K, 40–45 K and any combination between any two or three of them. That is, one always obtains step-like T_c's in the $La_2CuO_{4+\delta}$ system.

The reason for the stabilization of these phases may be the formation of some kind of ordered arrangement of the interstitial oxygen. Such a one-dimensional ordering of the extra oxygen along the *c*-axis is similar to the staging behavior of oxygened $La_2NiO_{4+\delta}$. The staging behavior in the $La_2CuO_{4+\delta}$ system has been observed and explained previously by Wells et al. [12,13] and Lee et al. [14,15]. The stage number *n* indicates that two consecutive interstitial layers are separated by $nCuO_2$ planes. At low oxygen content ($\delta = 0.01$–0.055), for which phase separate into oxygen-rich and oxygen-poor domains occurs, the oxygen-rich phase is stage-6 with a superconducting T_c of 30–32 K. In addition, it is reported that the phase stage-4 with $\delta = 0.11$ has the superconducting transition temperature $T_c =$ 40–45 K.

In addition to the staging structure, another oxygen ordering is the *ab*-plane oxygen ordering [16–18]. By electron diffraction, some superstructural modulation situated on the *ab*-plane was observed. For the 15 K phase, its depressed superconductivity possibly originates electronically from the *ab*-plane charge ordering which is compatible with the concept of the "stripe phase".

Previous studies mainly concentrated on the specimens obtained in the oxygen-increase process. We know that the excess oxygen will be lost during the thermal treatment process. Therefore, we can easily obtain samples with different oxygen content by thermal treatment to controllably reduce oxygen stoichiometries. In this work, the annealing behavior of the fully oxidized $La_2CuO_{4+\delta}$ in both structure and superconducting properties were monitored as annealed at 100 °C, 200 °C and 300 °C. The interrelation among the superconducting transition temperature T_c, structure, and thermal treatment temperature has been investigated and some interesting results have been found.

2. Experimental

Ceramic La_2CuO_4 was synthesized using the normal solid-state reaction from stoichiometric mixtures of La_2O_3 and CuO (Reagent Factory of Shanghai, China) with purity higher than 99.9%. La_2O_3 powder was calcined at 900 °C before weighting. The mixture of the starting materials was calcined at 900 °C and then 920 °C for 96 h totally with an intermediate grinding. The product was reground, palletized as discs, annealed at 960 °C for 72 h and oven cooled to room temperature in air. The specimens thus obtained were single-phase La_2CuO_4 as indicated by the power X-ray pattern.

The chemical oxidation of the stoichiometric La_2CuO_4 powder was performed using the following methods: about 10 g of the powder sample was put into the aqueous solution of NaClO (Xingfu Institute of fine Chemistry, Beijing, China), then was allowed to react at room temperature for 35 days. The aqueous solution of NaClO is volatile and was replaced frequently. The vessel full of La_2CuO_4 powder and NaClO solution was shaken periodically in order to assure identical intercalation of excess oxygen. After the oxidation treatment, the sample was filtered, washed with distilled water and ethanol, and dried on silica gel at room temperature. The cationic compositions of the dry samples estimated by ICP-AES were very close to the stoichiometric La_2CuO_4, and no foreign phases were detected by powder XRD analysis. Their orthorhombic room-temperature lattice parameters were $a = 5.342(6)$, $b = 5.370(1)$, $c = 13.226(9)$ Å, and $V = 379.479(6)$ Å^3 with superconducting transition temperature 40 K. The measured excess oxygen content corresponded to $\delta = 0.12 \pm 0.01$ using TGA analysis (Fig. 1). All the fully oxidized compounds were pressed into pellets with diameter 5 mm. These materials were subsequently thermal treated at 100 °C, 200 °C and 300 °C respectively in air for 1 min to 90 days followed by quenching to room temperature to controllably reduce oxygen stoichiometries.

X-ray powder diffraction was performed on MXP-AHF 18 diffractometer using Cu Kα radiation. The lattice parameters were calculated by

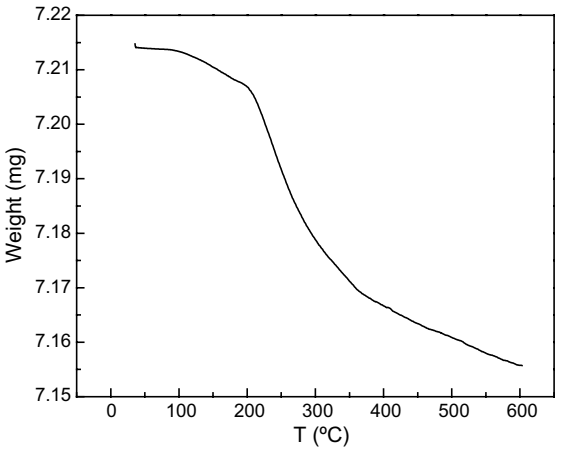

Fig. 1. TGA weight-loss curves for our fully oxidized $La_2Cu_{4+\delta}$ powder samples, in 1 atm dynamic air. The scan rate is 20 °C/min.

the least-squares method using the POWDERX program [19]. The magnetic measurements of the samples were carried out on a Quantum Design superconducting quantum interference device (SQUID) magnetometer. The superconducting transition temperature T_c has been measured in the field-cooled mode (Meissner signal) and the zero-field-cooled (shielding signal) mode were used to study the high-temperature magnetization property within the temperature range 5–300 K.

3. Results and discussion

Fig. 2 illustrates the sequence of successive structural transitions O → T → O (orthorhombic to tetragonal to orthorhombic) presented in our samples annealed at 200 °C. The labels of axis x correspond to the treatment time. The orthorhombic strain decreases and then increases with the increases of the oxygen content. The rough tendency of the structure variation is very similar to the result reported by Radaelli et al. and Lagueyte et al. [20,21].

Figs. 3–5 shows the temperature dependences of magnetization in the superconductivity onset region (a), and the corresponding derivative of M (b), for specimens annealed at 100 °C, 200 °C and 300 °C, respectively. The labels in the figure correspond to the treatment time. Each dM/dT curve is arbitrarily shifted vertically for clarity. Superconducting transition temperature T_c was defined by the onset of the magnetization

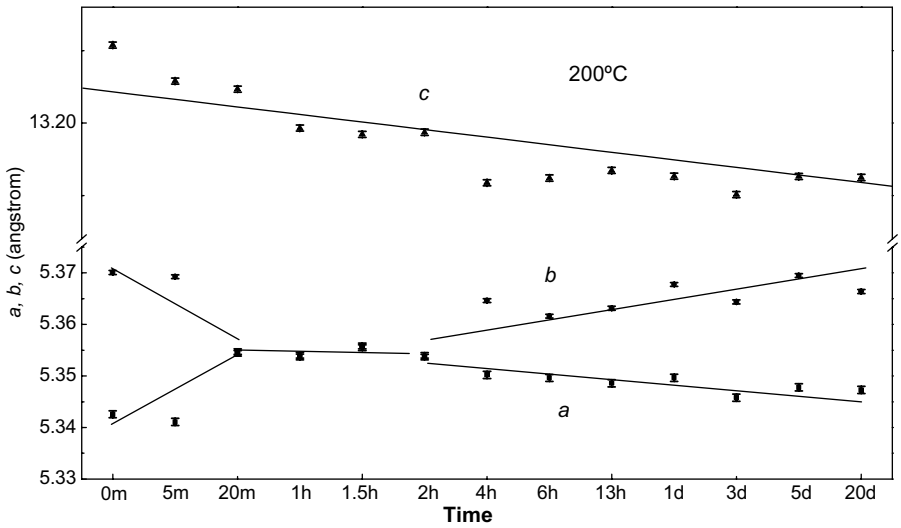

Fig. 2. The structure parameters a, b, and c as a function of annealing time determined by X-ray powder diffraction for samples annealed at 200 °C.

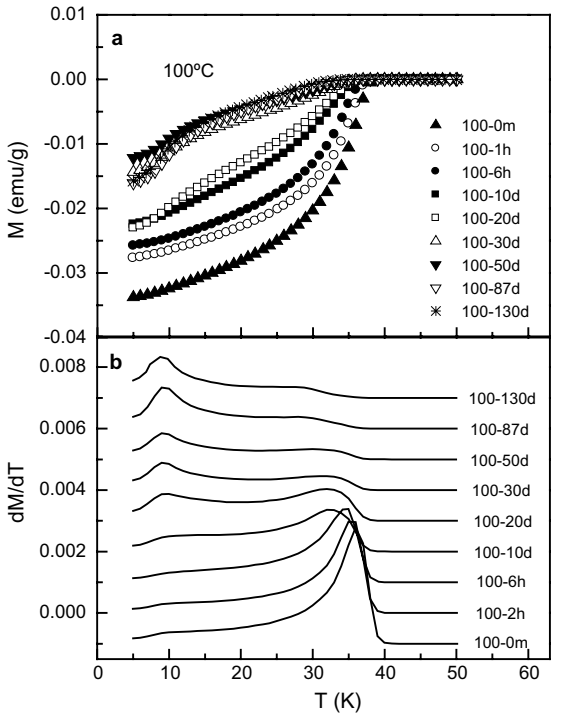

Fig. 3. Temperature dependences of magnetization in the superconductivity onset region (a), and the corresponding derivative of M (b), for specimens oxidized at 100 °C. The labels in the figure correspond to the treatment time.

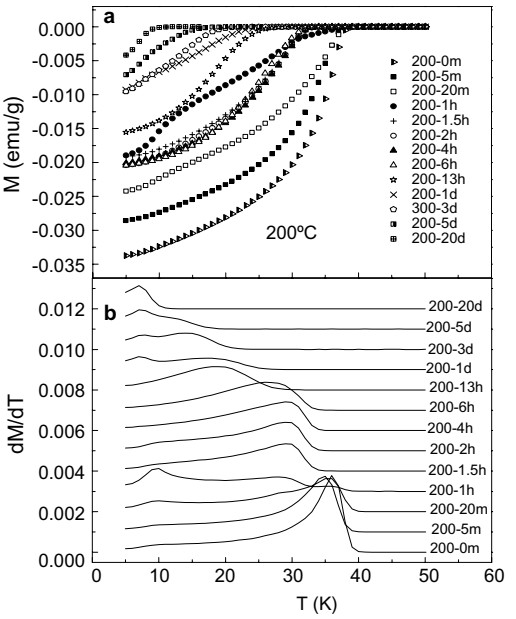

Fig. 4. Temperature dependences of magnetization in the superconductivity onset region (a), and the corresponding derivative of M (b), for specimens oxidized at 200 °C. The labels in the figure correspond to the treatment time.

transition, i.e. the corresponding temperature where the dM/dT curve begins to increase with the decrease of temperature.

For samples annealed at 100 °C, T_c keeps at 40 K at the beginning of the anneal until annealing time reach to 10 days, at which the sample separates into two superconducting phases with T_c's equal to 38 K and 15 K. By further annealing, the 15 K phase develops at the expense of 38 K phase. It seems that the 15 K phase is the most stable phase in this process. The typical step-like superconducting phases preserved in our samples are similar to the phase separation observed in the oxygen-increase process.

In the case of annealing at 200 °C, a single phase or multiphase mixture was obtained depending on different annealing time, as shown in Fig. 4. In addition to the 40 K superconducting transition, the 15 K and 34 K transitions develop after 20 min. Then the 40 K transition disappears when the annealing time reaches to 1 h. In the time range from 1.5 to 6 h, only the single transition 34 K can be detected. With further annealing, T_c decreases continuously and reaches to 10 K eventually.

It is well known that the coexistence of superconducting and antiferromagnetic phases is one characteristic feature of oxygen-doped $La_2CuO_{4+\delta}$ within the doping regime $0.01 < \delta < 0.055$. The antiferromagnetic transition is characterized by a well-defined peak at T_N (Néel temperature) following the Curie–Weiss-like behavior of magnetization with the decreasing of temperature.

In order to determine the magnetic nature of our samples, the higher-temperature (5–300 K) magnetization data for sample fully oxidized and sample with single superconductive phase $T_c \sim$ 34 K were collected, as shown in Fig. 6. The data for these two samples show no evidence of antiferromagnetic transition, indicating that no coexistence of superconductivity and the antiferromagnetism is present in our samples.

By increasing the anneal temperature to 300 °C, as displayed in Fig. 5, T_c decreases from 40 K to

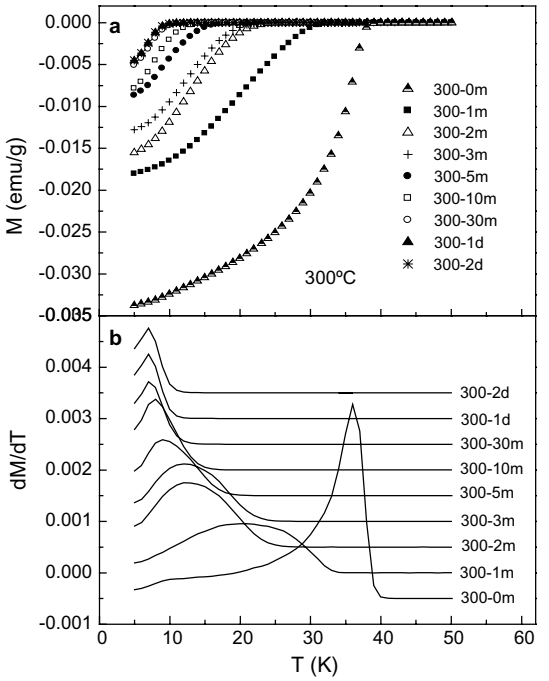

Fig. 5. Temperature dependences of magnetization in the superconductivity onset region (a), and the corresponding derivative of M (b), for specimens oxidized at 300 °C. The labels in the figure correspond to the treatment time.

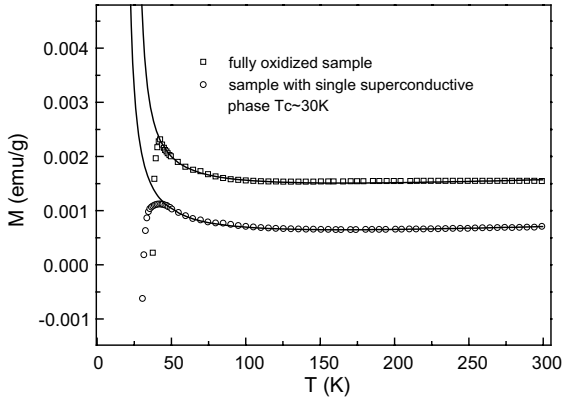

Fig. 6. High-temperature magnetization data for sample fully oxidized and sample with single superconductive phase $T_c \sim 30$ K under 5000 Oe.

10 K continuously as annealing time increases from 0 min to 1 day. Future treatment such as 2 days will not decrease T_c any more. Only one superconducting transition can be observed for all curves, which suggested that no phase separation occur through the thermal treatment process.

Feng et al. [5] found that $La_2CuO_{4+\delta}$ annealed at 100 °C do not lose oxygen no matter how long they annealed it. This is consistent with our data in Fig. 1. Therefore, we presume that the oxygen loss at 100 °C can be neglected. With the prolonging of the anneal time, the mobile oxygen will participate in the system's thermodynamics, arranging themselves so as to minimize the free energy to the extent their mobility permits. Therefore, the appearance of the discontinuous T_c phases upon annealing are due to thermally activated rearrangements of interstitial oxygen atoms in the lattice with the formation of different superconducting domains, like the stage structures.

The time dependence of Meissner fraction of samples annealed at 100 °C is shown in Fig. 7. The Meissner fraction decreases continuously until annealing time reaches to 30 days, after that it keeps constant. Since no loss of oxygen is expected at 100 °C, the continuous reduction of the Meissner fraction upon annealing are due to thermally activated rearrangements of interstitial oxygen atoms with the formation of different superconducting domains. With the formation of the stable 15 K phase when annealing time reaches to 30 days, the Meissner fraction reaches a constant.

In the case of 300 °C treatment, the interstitial oxygen atoms move quickly in the lattice in that they cannot reorder into an equilibrium

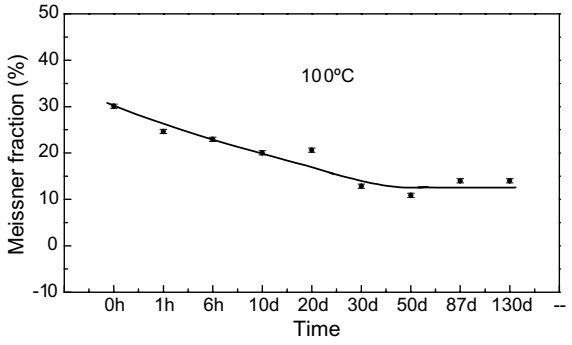

Fig. 7. Time dependence of Meissner fraction of samples annealed at 100 °C.

arrangement when we quench the samples from the furnace quickly. This means that the oxygen is homogeneously distributed and acts as a local dopant in a manner similar to strontium in $La_{2-x}Sr_xCuO_4$. On the other hand, the excess oxygen content will decrease in the annealing process at 300 °C (see Fig. 1), so the stoichiometries can be adjusted to produce any T_c between 45 K and 10 K with the increasing of annealing time. This is consistent with our observation of the continuously decreased T_c.

The variation of Meissner fraction as a function of annealing time of samples annealed at 300 °C is shown in Fig. 8. The Meissner fraction decreases monotonously with annealing. Only single superconductive phase can be obtained through the whole annealing process. The drastic reduction of the Meissner fraction upon annealing is, therefore, due to the continuous loss of the oxygen.

Annealing at 200 °C, oxygen content will decrease also, but the kinetics is substantially slower than that at 300 °C. The continuous decrease of T_c is approached after annealing for 6 h. According to our analysis, it is easy to understand that we get the discontinuous T_c at the beginning of the treatment and then T_c decreases continuously.

The time dependence of Meissner fraction of samples annealed at 200 °C is shown in Fig. 9. It should be noticed that with the appearance of single transition 34 K phase, the Meissner fraction keeps stable from 1.5 to 6 h. This indicates that the conversion to the 34 K phase corresponds to a low activation energy. Therefore, we suppose that the 34 K phase is a stable phase and can be obtained easily, as reported [1–11].

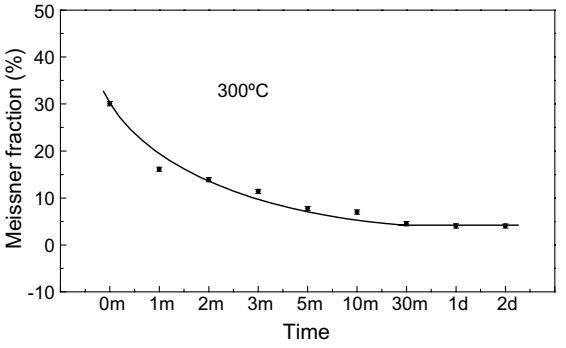

Fig. 8. Time dependence of Meissner fraction of samples annealed at 300 °C.

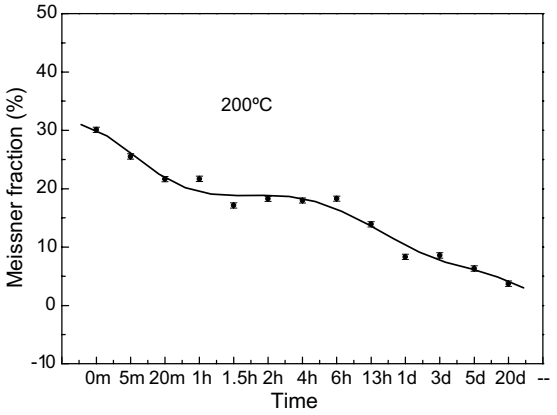

Fig. 9. Time dependence of Meissner fraction of samples annealed at 200 °C.

4. Conclusion

In this paper, superconductive $La_2CuO_{4+\delta}$ with $T_c \sim 40$ K has been obtained by chemical oxidation using NaClO solution. We treated them in furnace under different temperature and studied the oxygen-decrease process. The magnetic measurements performed on our samples give out remarkable features that are different from those already reported for $La_2CuO_{4+\delta}$ in the oxygen-increase process. The evolution of the superconducting transition temperature T_c with time is different at different annealing temperature: (i) step-like behavior is observed at 100 °C; (ii) both step and continuous T_c appear with the prolonging of the annealing time at 200 °C; (iii) T_c decreases continuously at 300 °C. In addition, we cannot observe the coexistence of superconducting and antiferromagnetic phases in our samples.

References

[1] F.C. Chou, D.C. Johnston, Phys. Rev. B 54 (1996) 572.
[2] F.C. Chou, J.H. Cho, D.C. Johnston, Physica C 197 (1992) 303.

[3] J.D. Jorgensen, B. Dabrowski, S. Pei, D.G. Hinks, L. Soderholm, B. Morosin, J.E. Schirber, E.L. Venturini, D.S. Ginley, Phys. Rev. B 38 (1988) 11337.
[4] J.-C. Grenier, N. Lagueyte, A. Wattiaux, J.-P. Doumerc, P. Dordor, J. Etourneau, M. Pouchard, J.B. Goodenough, J.S. Zhou, Physica C 202 (1992) 209.
[5] H.H. Feng, Z.G. Li, P.H. Hor, S. Bhavaraju, J.F. DiCarlo, A.J. Jacobson, Phys. Rev. B 51 (1995) 16499.
[6] P.H. Hor, H.H. Feng, Z.G. Li, J.F. Dicarlo, S. Bhavaraju, A.J. Jacobson, J. Phys. Chem. Solids 57 (1996) 1061.
[7] L. Chen, C. Dong, Y.Z. Huang, F. Zhou, G.C. Che, Z.X. Zhao, Solid State Commun. 114 (2000) 107.
[8] Q.Y. Tu, X.L. Chen, B.K. Ma, Z.X. Zhao, J.Q. Li, J.K. Liang, Physica C 370 (2002) 94.
[9] E. Takayama-Muromachi, T. Sasaki, Y. Matsui, Physica C 207 (1993) 97.
[10] E. Takayama-Muromachi, A. Navrotsky, Physcia C 218 (1993) 164.
[11] Toshikazu Hirayama, Masahito Nakagawa, Akihiko Sumiyama, Yasukage Oda, Phys. Rev. B 58 (1998) 5856.
[12] B.O. Wells, Y.S. Lee, M.A. Kastner, R.J. Christianson, R.J. Birgeneau, K. Yamada, Y. Endoh, G. Shirane, Science 277 (1997) 1067.
[13] B.O. Wells, R.J. Birgeneau, F.C. Chou, Y. Endoh, D.C. Johnston, M.A. Kastner, Y.S. Lee, G. Shirane, J.M. Tranquada, K. Yamada, Z. Phys. B 100 (1996) 535.
[14] Y.S. Lee, R.J. Birgeneau, M.A. Kasner, Phys. Rev. B 60 (1999) 3643.
[15] A.T. Savici, Y. Fudamoto, I.M. Gat, T. Ito, M.I. Larkin, Y.J. Uemura, G.M. Luke, K.M. Kojima, Y.S. Lee, M.A. Kastner, R.J. Birgeneau, K. Yamada, Phys. Rev. B 66 (2002) 014524.
[16] G.D. Liu, Min Gao, G.C. Che, Z.X. Zhao, L. Chen, C. Dong, F. Wu, Y.M. Ni, H. Chen, L.M. Peng, Supercond. Sci. Technol. 14 (2001) 398.
[17] C.H. Chen, S.-W. Cheong, A.S. Cooper, Phys. Rev. Lett. 71 (1993) 2461.
[18] J.M. Tranquada, J.D. Axe, N. Ichikawa, A.R. Moodenbaugh, Y. Nakamura, S. Uchida, Phys. Rev. Lett. 78 (1997) 338.
[19] C. Dong, J. Appl. Crystallogr. 32 (1999) 838.
[20] P.G. Radaelli, J.D. Jorgensen, A.J. Schultz, B.A. Hunter, J.L. Wagner, F.C. Chou, D.C. Johnston, Phys. Rev. B 48 (1993) 499.
[21] N. Lagueyte, A. Wattiaux, J.C. Park, J.-C. Grenier, L. Fournes, M. Pouchard, J. Phys. III 1 (1991) 1755.